Supplementary material for "A sub-asymptotic model for bivariate threshold exceedances"

Mirco Lescart* Anna Kiriliouk* Philippe Naveau†

May 11, 2026

A.1 Additional proofs

Proof of Lemma 8.1.

1. For $w \in (0,1)$, the numerator $N = wE + (1-w)E_j$ of V_j is a sum of two independent exponential variables with different scale parameters. Its distribution is hypo-exponential with cdf
$$F_N(u) = 1 - \frac{(1-w)e^{-u/w} - we^{-u/(1-w)}}{2w-1}.$$
Let f_{G+G_j} denote the density of $G + G_j \sim \Gamma(1/\xi_j, 1)$. Straightforward calculations give the cdf of $V_j = N/(G+G_j)$, for $x \geq 0$,
$$\begin{aligned} F_{V_j}(x) = \mathbb{P}(V_j \leq x) &= \int_0^\infty F_N(xt) \cdot f_{G+G_j}(t)\ \mathrm{d}t \\ &= 1 - \frac{w(1+\frac{x}{w})^{-1/\xi_j} - (1-w)(1+\frac{x}{1-w})^{-1/\xi_j}}{2w-1}. \end{aligned} \tag{A.1}$$
Differentiating (A.1) with respect to x yields the stated density. The cases $w \in \{0,1\}$ can be obtained directly from Lemma 2.1. The expression for $w = \frac{1}{2}$ can be obtained by applying l'Hôpital's rule to the above formula.

2. The mean and variance follow from the facts that, writing $V_j = NM$ for $M = (G+G_j)^{-1}$,
$$\begin{aligned} \mathbb{E}[N] &= 1, & \mathbb{E}[N^2] &= 1 + w^2 + (1-w)^2, \\ \mathbb{E}[M] &= \frac{1}{\xi_j^{-1} - 1}, & \mathbb{E}[M^2] &= \frac{1}{(\xi_j^{-1}-1)(\xi_j^{-1}-2)}. \end{aligned}$$

□

*LIDAM/ISBA, UCLouvain, Voie du Roman Pays 20, 1348 Louvain-la-Neuve, Belgium. E-mails: mirco.lescart@uclouvain.be, anna.kiriliouk@uclouvain.be

†Laboratoire des Sciences du Climat et de l'Environnement (IPSL, CNRS, CEA, UVSQ). E-mail: naveau@lsce.ipsl.fr

Proof of Lemma 8.2. For $\lambda > 0$ and $\alpha > 0$, we have

$$\frac{(1+\lambda x)^{-\alpha}}{(\lambda x)^{-\alpha}} = 1 - \alpha(\lambda x)^{-1} + o(x^{-1}), \qquad \text{as } x \to \infty. \tag{A.2}$$

Expanding $(1+\lambda x)^{-1/\xi_j}$ in (A.1) according to (A.2) for $\lambda = 1/w$ and $\lambda = 1/(1-w)$ and collecting constants, we get

$$\overline{F}_{V_j}(x) = Cx^{-1/\xi_j}\left(1 - \frac{D}{\xi_j x} + o(x^{-1})\right), \qquad \text{as } x \to \infty,$$

for $w \in [0,1] \setminus \{\frac{1}{2}\}$, where C and D are given in (8.2). When $w = \frac{1}{2}$, l'Hôpital's rule gives

$$C = 2^{-1/\xi_j}(\xi_j^{-1} + 1) \quad \text{and} \quad D = \frac{1+2\xi_j}{2+2\xi_j}.$$

□

Proof of Lemma 8.3. We write

$$\mathbb{P}\left[V_1 > x_1, V_2 > x_2\right] = \mathbb{P}\left[E > \max_{j=1,2}\left\{\frac{x_j(G+G_j) - (1-w)E_j}{w}\right\}\right].$$

Conditioning on all variables except E and defining $M_j := x_j(G+G_j) - (1-w)E_j$, we obtain

$$\mathbb{P}(V_1 > x_1, V_2 > x_2) = \mathbb{E}\left[e^{-(M_1 \vee M_2)/w}\mathbb{1}\{M_1 \vee M_2 > 0\}\right] + \mathbb{P}\{M_1 \vee M_2 < 0\}.$$

Decomposing on $\{M_1 > M_2\}$ and $\{M_2 \geq M_1\}$ yields

$$\mathbb{P}(V_1 > x_1, V_2 > x_2) = A_1 + A_2 + A_{12},$$

with $A_{12} = \mathbb{P}\{M_1 \vee M_2 < 0\}$,

$$A_1 = \mathbb{E}\left[e^{-M_1/w}\mathbb{1}\{M_1 > M_2 \vee 0\}\right], \text{ and } A_2 = \mathbb{E}\left[e^{-M_2/w}\mathbb{1}\{M_2 > M_1 \vee 0\}\right].$$

Term A_{12}: Since $M_1 \vee M_2 < 0$ iff $(1-w)E_j > x_j(G+G_j)$ for $j = 1, 2$, conditioning on (G, G_1, G_2) and using independence of exponentials gives

$$A_{12} = \mathbb{E}\left[e^{-\frac{x_1+x_2}{1-w}G}e^{-\frac{x_1}{1-w}G_1}e^{-\frac{x_2}{1-w}G_2}\right].$$

Applying the Laplace transform of Gamma variables yields

$$A_{12} = \left(1 + \frac{x_1+x_2}{1-w}\right)^{-\alpha}\left(1 + \frac{x_1}{1-w}\right)^{-\alpha_1}\left(1 + \frac{x_2}{1-w}\right)^{-\alpha_2}.$$

Term A_1: Using $M_j = x_j(G+G_j) - (1-w)E_j$, we write

$$A_1 = \mathbb{E}\left[e^{-\frac{x_1}{w}(G+G_1)}e^{\frac{1-w}{w}E_1}\mathbb{1}\{M_1 > M_2,\ M_1 > 0\}\right].$$

The constraints are equivalent to $E_1 \le B$, where

$$B = \min\left\{ \frac{x_1}{1-w}(G+G_1),\ \frac{x_1}{1-w}(G+G_1) + E_2 - \frac{x_2}{1-w}(G+G_2) \right\}.$$

Conditioning on all variables except E_1 and evaluating the exponential integral (valid for $w \neq \frac{1}{2}$) yields

$$A_1 = \frac{w}{1-2w}\,\mathbb{E}\left[e^{-\frac{x_1}{w}(G+G_1)} \left(e^{\frac{1-2w}{w} B_+} - 1 \right) \right], \qquad B_+ = \max(B, 0).$$

Introduce the rescaled variables $\tilde{G} = \frac{w}{x_1+w} G$ and $\tilde{G}_1 = \frac{w}{x_1+w} G_1$. Using scaling invariance of Gamma distributions,

$$A_1 = \frac{w}{1-2w} \left(1 + \frac{x_1}{w} \right)^{-(\alpha+\alpha_1)} \mathbb{E}\left[e^{\frac{1-2w}{w} \tilde{B}_+} - 1 \right],$$

where $\tilde{B}$ denotes the corresponding rescaled bound. Since the integrand vanishes on $\{\tilde{B} \le 0\}$,

$$\mathbb{E}\left[e^{\frac{1-2w}{w} \tilde{B}_+} - 1 \right] = \mathbb{E}\left[(e^{\frac{1-2w}{w} \tilde{B}_+} - 1) \mathbb{1}\{\tilde{B} > 0\} \right].$$

Conditioning on (G, G_1, E_2) and integrating out G_2 gives

$$A_1 = \frac{w(1-w)^{\alpha_2}}{1-2w} \left(1 + \frac{x_1}{w} \right)^{-(\alpha+\alpha_1)} x_2^{-\alpha_2}\, \mathbb{E}[\mathcal{I}_1], \tag{A.3}$$

where $\mathcal{I}_1$ is the integral term

$$\mathcal{I}_1 = \int_0^{H_1} \left(\exp\left(\frac{1-2w}{w} \min\{\tilde{D}_1,\, H_1 - y\} \right) - 1 \right) \frac{y^{\alpha_2 - 1}}{\Gamma(\alpha_2 + 1)} \exp\left(-\frac{1-w}{x_2} y \right) dy,$$

with

$$\tilde{D}_1 = \frac{x_1 w}{(1-w)(x_1+w)}(G+G_1), \qquad H_1 = \tilde{D}_1 + E_2 - \frac{x_2 w}{(1-w)(x_1+w)} G.$$

Term A_2: The expression for A_2 follows by symmetry after exchanging indices 1 and 2.

Combining A_1, A_2 and A_{12} yields the stated survival function. □

Proof of Lemma 8.4. Let $(x_1, x_2) = (u_1(q), u_2(q))$ with $q \uparrow 1$. Since V_j has a GP tail (see the proof of Proposition 3.2 (iii)), it is regularly varying with index $\alpha + \alpha_j$, hence for some constants $C_j > 0$,

$$u_j(q) := F_{V_j}^{-1}(q) \sim C_j\, (1-q)^{-1/(\alpha+\alpha_j)}, \qquad q \uparrow 1,$$

and therefore $u_j(q)^{-\beta} \sim C_j^{-\beta}\, (1-q)^{\beta/(\alpha+\alpha_j)}$ for any $\beta > 0$. In particular, assume without loss of generality that $\alpha_1 < \alpha_2$, in which case $u_2(q)/u_1(q) \to 0$. We analyse successively the three contributions A_1, A_2, A_{12} from

$$\mathbb{P}(V_1 > x_1, V_2 > x_2) = A_1(x_1, x_2) + A_2(x_1, x_2) + A_{12}(x_1, x_2),$$

obtained in Lemma 8.3.

Contribution of A_{12}: Using $(1+x/a)^{-k} \sim (x/a)^{-k}$ and $x_1 + x_2 \sim x_1$, we obtain

$$A_{12}(x_1, x_2) \sim (1-w)^{\alpha+\alpha_1+\alpha_2}\, x_1^{-(\alpha+\alpha_1)} x_2^{-\alpha_2} \sim c_{12}\,(1-q)^{\,1+\frac{\alpha_2}{\alpha+\alpha_2}},$$

for some constant $c_{12} \in (0, \infty)$.

Contribution of A_1: From (A.3) and $(1+x_1/w)^{-(\alpha+\alpha_1)} \sim w^{\alpha+\alpha_1} x_1^{-(\alpha+\alpha_1)}$, we get

$$A_1(x_1, x_2) \sim K_1\, x_1^{-(\alpha+\alpha_1)} x_2^{-\alpha_2}\, \mathbb{E}\left[\mathcal{I}_1(x_1, x_2)\right], \qquad K_1 := \frac{w(1-w)^{\alpha_2}}{1-2w}\, w^{\alpha+\alpha_1}.$$

In the regime $x_1, x_2 \to \infty$ with $x_2/x_1 \to 0$, $\mathcal{I}_1(x_1, x_2) \to \mathcal{I}_{1,\infty}$ a.s. and is dominated by an integrable envelope (Gamma moments), so dominated convergence yields $\mathbb{E}[\mathcal{I}_1(x_1, x_2)] \to \kappa_1 \in (0, \infty)$. Consequently,

$$A_1(x_1, x_2) \sim c_1\, x_1^{-(\alpha+\alpha_1)} x_2^{-\alpha_2} \sim c_1\,(1-q)^{\,1+\frac{\alpha_2}{\alpha+\alpha_2}},$$

for some $c_1 \in (0, \infty)$.

Contribution of A_2: By symmetry (swap indices 1 and 2 in (A.3)),

$$A_2(x_1, x_2) = \frac{w(1-w)^{\alpha_1}}{1-2w} \left(1 + \frac{x_2}{w}\right)^{-(\alpha+\alpha_2)} x_1^{-\alpha_1}\, \mathbb{E}[\mathcal{I}_2(x_1, x_2)].$$

In the regime $x_1, x_2 \to \infty$ with $x_2/x_1 \to 0$, the constraint defining $\mathcal{I}_2$ forces $G = O(x_2/x_1)$; with the scaling $G = (x_2/x_1)U$ and the small-argument expansion of the Gamma density, one obtains

$$\mathbb{E}[\mathcal{I}_2(x_1, x_2)] \sim \kappa_2 \left(\frac{x_2}{x_1}\right)^{\alpha}, \qquad \kappa_2 \in (0, \infty),$$

and therefore

$$A_2(x_1, x_2) \sim c_2\, x_1^{-(\alpha+\alpha_2)} x_2^{-\alpha_1} \sim c_2\,(1-q)^{\,1+\frac{\alpha_2}{\alpha+\alpha_2}},$$

for some $c_2 \in (0, \infty)$.

If $\alpha_1 > \alpha_2$, the same expansions hold with the roles of α_1 and α_2 reversed. Hence, we find

$$\bar{F}_{V_1,V_2}\left(u_1(q), u_2(q)\right) \sim (c_1 + c_2 + c_{12})\,(1-q)^{\,1+\frac{\max(\alpha_1,\alpha_2)}{\alpha+\max(\alpha_1,\alpha_2)}}. \tag{A.4}$$

□

Proof of Lemma 8.5. Since V_j is regularly varying and $S_j \geq 0$, by dominated convergence, we have $\bar{F}_{Y_j}(x) = \bar{F}_{V_j}(x)(1+o(1))$ as $x \to \infty$. By Resnick (2007, Proposition 2.6(vi)), this yields $w_j(q) := F_{Y_j}^{-1}(q) = F_{V_j}^{-1}(q)(1+o(1))$ as $q \uparrow 1$. From the proof of Lemma 8.4, recall that $u_j(q) := F_{V_j}^{-1}(q) \sim C_j(1-q)^{-1/(\alpha+\alpha_j)}$. In particular, the proof of Lemma 8.4 gives

$$\bar{F}_{V_1,V_2}\left(u_1(q)\{1+o(1)\}, u_2(q)\{1+o(1)\}\right) \sim \bar{F}_{V_1,V_2}\left(u_1(q), u_2(q)\right) \tag{A.5}$$

Next, note that

$$\bar{F}_{Y_1,Y_2}(w_1(q), w_2(q)) = \mathbb{E}\left[\bar{F}_{V_1,V_2}(w_1(q) + S_1,\ w_2(q) + S_2)\right].$$

Define

$$R(q) := \frac{\bar{F}_{V_1,V_2}(w_1(q) + S_1,\ w_2(q) + S_2)}{\bar{F}_{V_1,V_2}(w_1(q), w_2(q))}.$$

Conditionally on (S_1, S_2), the shifts become deterministic constants. Since $w_j(q) \to \infty$, we have $S_j = o(w_j(q))$ a.s., so that equation A.5 yields $R(q) \to 1$ almost surely. Moreover, since $0 \leq R(q) \leq 1$, we have $\mathbb{E}[R(q)] \to 1$ by bounded convergence and

$$\bar{F}_{Y_1,Y_2}(w_1(q), w_2(q)) \sim \bar{F}_{V_1,V_2}(w_1(q), w_2(q)), \qquad q \uparrow 1.$$

Finally, using again equation A.5,

$$\bar{F}_{Y_1,Y_2}(F_{Y_1}^{-1}(q), F_{Y_2}^{-1}(q)) \sim \bar{F}_{V_1,V_2}\left(F_{V_1}^{-1}(q), F_{V_2}^{-1}(q)\right), \qquad q \uparrow 1.$$

so that dividing by $(1-q)$ and letting $q \uparrow 1$ gives $\chi_{\boldsymbol{Y}} = \chi_{\boldsymbol{V}}$. If $\chi_{\boldsymbol{V}} = 0$, then taking logarithms gives also $\eta_{\boldsymbol{Y}} = \eta_{\boldsymbol{V}}$. □

A.2 Simulation Study: additional results

This appendix provides additional simulation results that complement the analysis in Section 5. We report results under randomized parameter configurations, as well as results for the penalized estimator in the fixed-parameter setting.

A.2.1 Randomized parameters

We assess the global performance of the NBE under randomly generated parameter configurations. For each of the $K = 10^3$ replications, we draw the parameters

$$(\eta, \xi_1, \xi_2, \beta_1, \beta_2, \sigma_T, w)$$

independently from their prior distributions specified in Section 4. The values of η, ξ_1 and ξ_2 are then transformed into the model parameters $(\alpha, \alpha_1, \alpha_2)$ according to the construction described in Section 3.1, and a dataset of size $N = 1000$ is simulated from the resulting model. Each dataset is then provided to the NBE for estimation.

Figure A.1 compares true and estimated values for all parameters. The points cluster tightly around the diagonal, indicating accurate recovery of both the model parameters and the extremal dependence structure. Estimates of η exhibit higher variability for lower values, and stabilize as η increases. This pattern is expected since weaker dependence (smaller η) corresponds to lighter joint tails, providing less information for reliable estimation. In contrast, when η approaches 1, the stronger dependence structure yields more stable and precise estimates across replications.

A.2.2 Simulation study: Penalised NBE (fixed-parameter setting)

In Figures A.2 and A.3 and Table A.1, we report additional results for the fixed-parameter simulation setting using the penalized NBE. The experimental design is identical to that described in Section 5, with the only difference being the use of the penalized loss function.

Overall, the penalised NBE introduces small biases, leading to a moderate reduction in coverage for several parameters, in particular (η, ξ_1, ξ_2) and σ_T. This effect is more pronounced

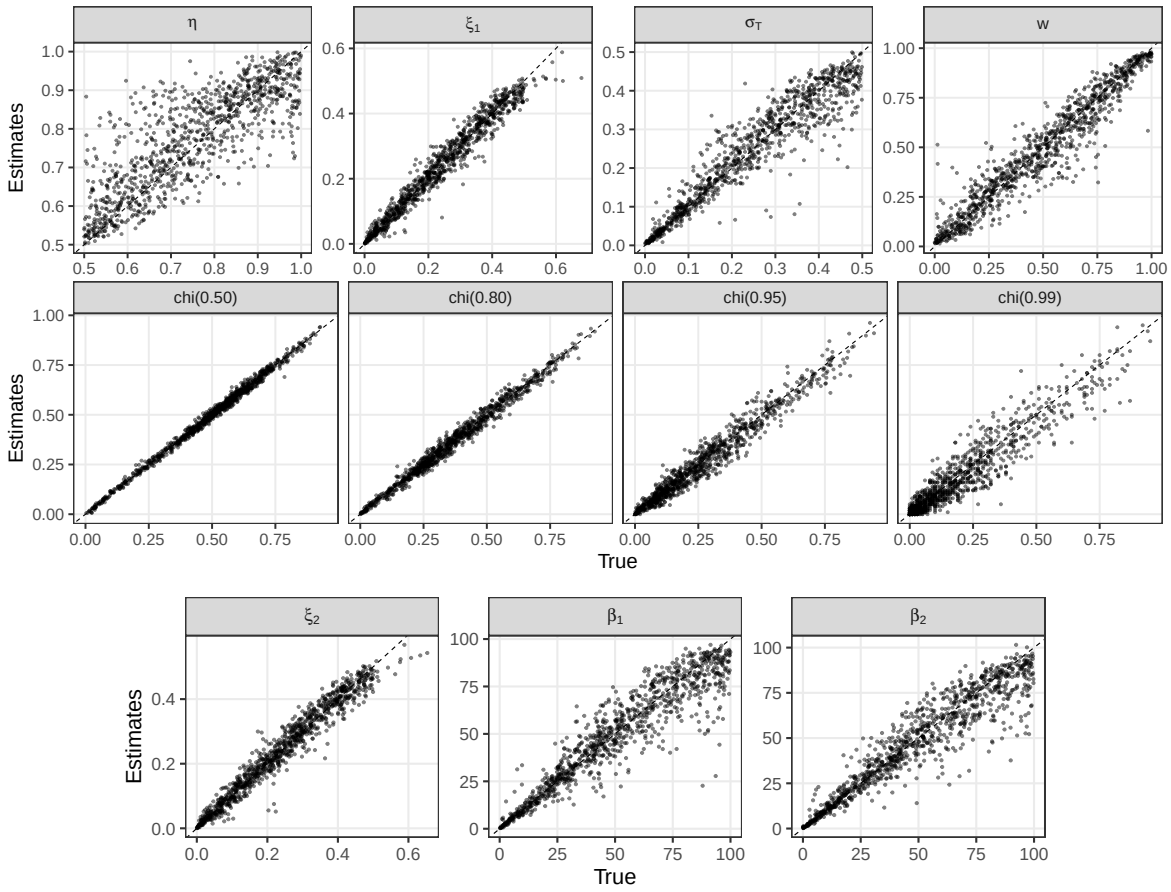

Figure A.1: True vs estimated values for η, ξ_1, σ_T, w (top), $\chi(q)$ with $q \in \{0.5, 0.8, 0.95, 0.99\}$ (middle), and ξ_2, β_1, β_2 (bottom) in the randomized parameter setting with $n = 1000$. Each point corresponds to one of the $K = 1000$ Monte Carlo replications.

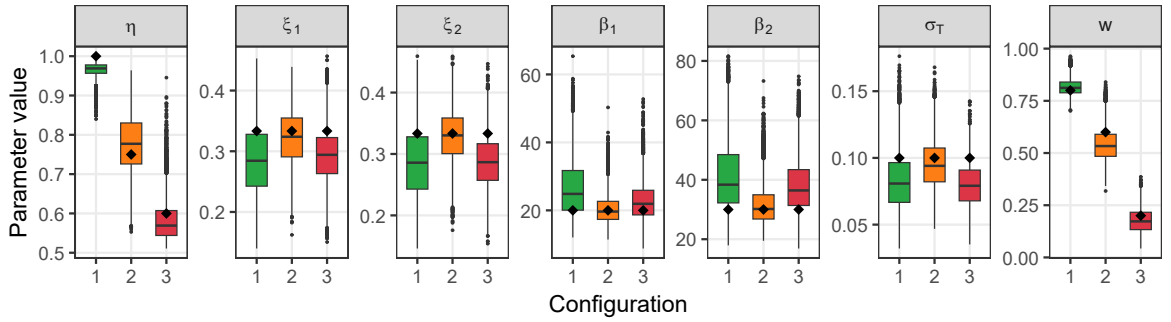

Figure A.2: Boxplots of parameter estimates $(\eta, \xi_1, \xi_2, \beta_1, \beta_2, \sigma_T, w)$ obtained with the penalised NBE under three dependence configurations: $\boldsymbol{\theta}^{(1)}$, $\boldsymbol{\theta}^{(2)}$, and $\boldsymbol{\theta}^{(3)}$ (see (5.1)), based on $K = 1000$ samples of size $N = 1000$. Diamond markers indicate true values.

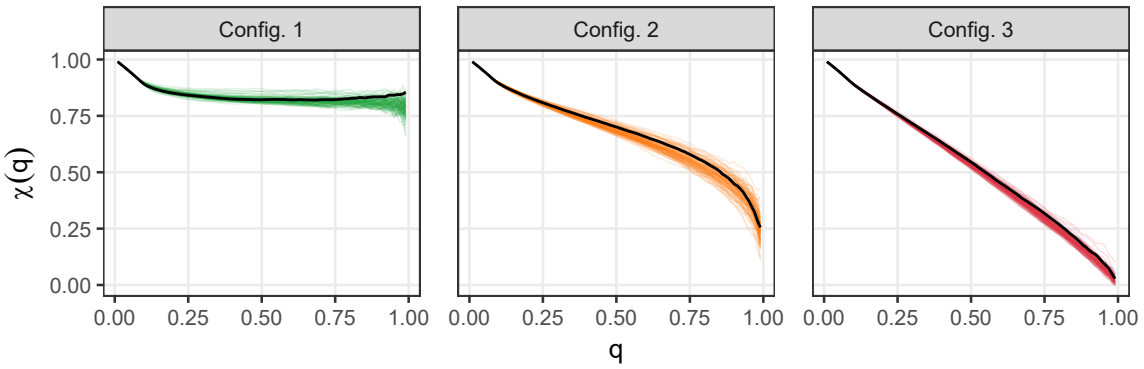

Figure A.3: Estimated $\chi(q)$ curves obtained with the penalised NBE, where $\chi(q)$ is estimated using (3.5). Solid lines correspond to reference curves empirically estimated from samples of size 10^5 generated under the true parameters. Coloured lines show 100 estimated curves based on samples of size 10^4 generated under fitted parameter values.

	Config. 1			Config. 2			Config. 3		
$\hat{\theta}_j$	True	Cov.	Width	True	Cov.	Width	True	Cov.	Width
$\hat{\eta}$	1.00	0.00	0.05	0.75	0.90	0.20	0.60	0.86	0.14
$\hat{\xi}_1$	0.33	0.73	0.15	1.50	0.89	0.11	0.33	0.68	0.12
$\hat{\xi}_2$	0.33	0.72	0.15	1.50	0.90	0.11	0.33	0.69	0.12
$\hat{\beta}_1$	20.00	0.79	20.9	20.00	0.96	10.8	20.00	0.87	15.2
$\hat{\beta}_2$	30.00	0.63	28.8	30.00	0.94	17.1	30.00	0.76	23.5
$\hat{\sigma}_T$	0.10	0.78	0.06	0.10	0.89	0.04	0.10	0.59	0.04
$\hat{w}$	0.80	0.86	0.10	0.60	0.78	0.21	0.20	0.92	0.15
$\chi(0.50)$	0.82	1.00	0.05	0.70	1.00	0.05	0.55	1.00	0.04
$\chi(0.70)$	0.82	1.00	0.06	0.60	1.00	0.08	0.37	1.00	0.06
$\chi(0.80)$	0.83	1.00	0.06	0.54	1.00	0.11	0.27	1.00	0.06
$\chi(0.90)$	0.84	1.00	0.07	0.45	1.00	0.13	0.16	1.00	0.07
$\chi(0.95)$	0.84	0.77	0.09	0.37	1.00	0.16	0.10	1.00	0.07
$\chi(0.99)$	0.85	0.51	0.16	0.23	1.00	0.22	0.03	1.00	0.06

Table A.1: Empirical coverage probability (Cov.) and mean confidence interval width (Width) for model parameters and tail dependence curves $\chi(q)$ obtained with the penalised NBE under three fixed configurations defined in (5.1) ($N = 1000$, $K = 1000$, $B = 200$ bootstrap resamples per estimate), together with the true values.

in the weakest dependence setting (Config. 3). In contrast, the estimation of $\chi(q)$ remains stable across most quantiles, with coverage close to the nominal level, except at the most extreme levels (e.g., $q = 0.99$ in Config. 1). These results highlight a trade-off induced by penalisation: improved structural coherence of the estimates at the cost of a modest loss in estimation quality due to the introduction of small biases.

A.3 Application to Belgian Weekly Rainfall: additional results

A.3.1 Parameter stability and QQ-plots

We present some supplementary figures for the Belgian rainfall application.

Figure A.4 shows the spatial domain used in the analysis, corresponding to all ERA5 grid points in the rectangle $[0^\circ, 7^\circ]\text{E} \times [47^\circ, 52^\circ]\text{N}$. The central reference grid point covering Brussels is marked, along with neighbouring points. Coordinates correspond to the centres of the ERA5 grid cells.

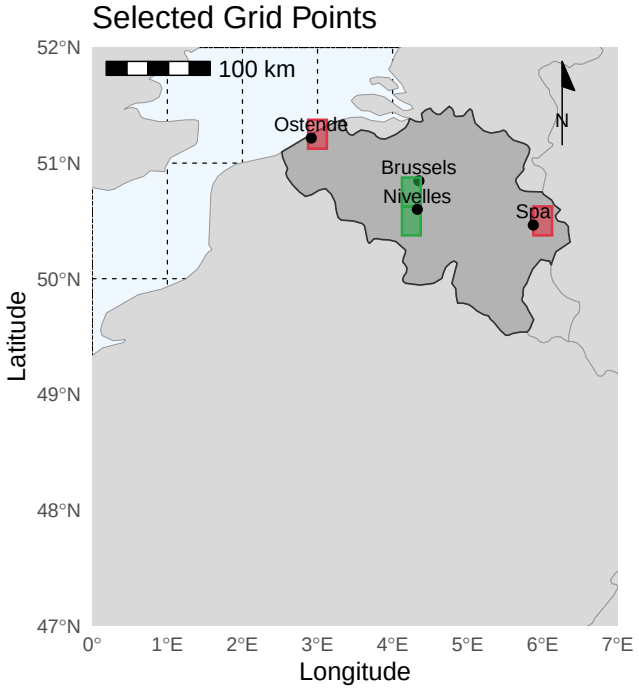

Figure A.4: Reference grid point (black point, Brussels) and surrounding ERA5 grid points within the analysis domain $[0^\circ, 7^\circ]\text{E} \times [47^\circ, 52^\circ]\text{N}$. Coordinates indicate grid cell centres.

Next, Figure A.5 reports parameter estimates as functions of the marginal threshold, for all pairs involving the Brussels reference grid point. These plots provide a visual check of threshold stability for both marginal and dependence parameters.

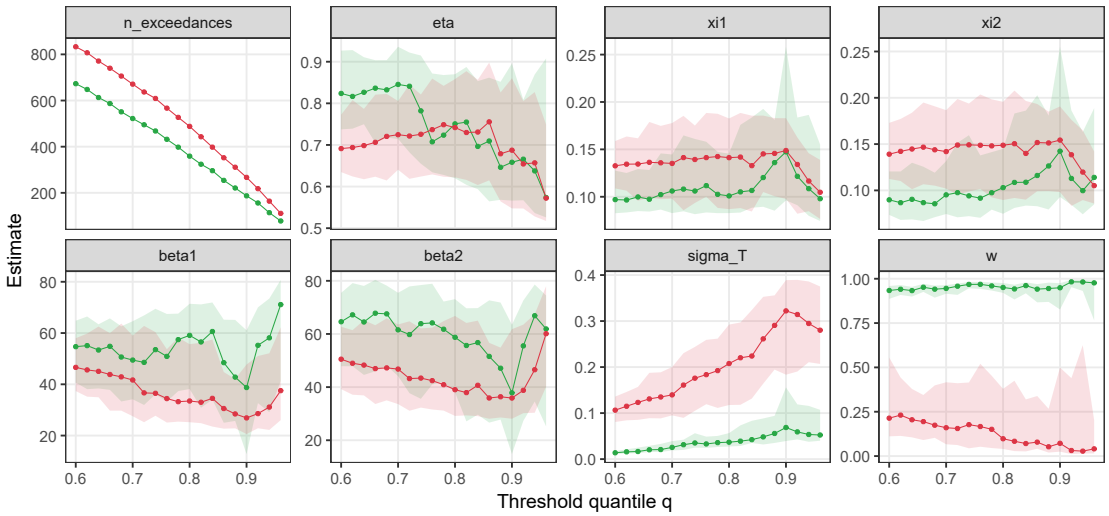

Figure A.5: Estimated parameter values of the sBGP model (Definition 3.1) as a function of the threshold quantile q for Brussels–Nivelles and Ostend–Spa. Green corresponds to the Brussels–Nivelles pair and red to the Ostend–Spa pair. Shaded areas denote the 95% bootstrap confidence intervals.

Finally, Figure A.6 complements Figure 8 in the main paper, illustrating several additional parameters as spatial fields.

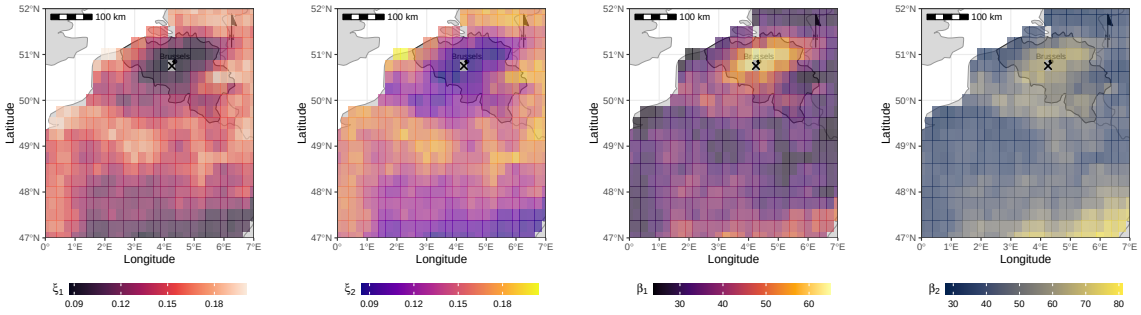

Figure A.6: Spatial fields of estimated parameters of the sBGP model (Definition 3.1) for bivariate precipitation extremes between Brussels (reference location, black cross) and each grid point.

A.3.2 Non-Penalised NBE

Figure A.7 shows the spatial fields of estimated parameters for the Belgian rainfall application obtained using the NBE trained without penalisation. These results are provided for comparison with the penalised version discussed in the main text, and illustrate the impact of the loss specification on both parameter estimates and goodness-of-fit diagnostics.

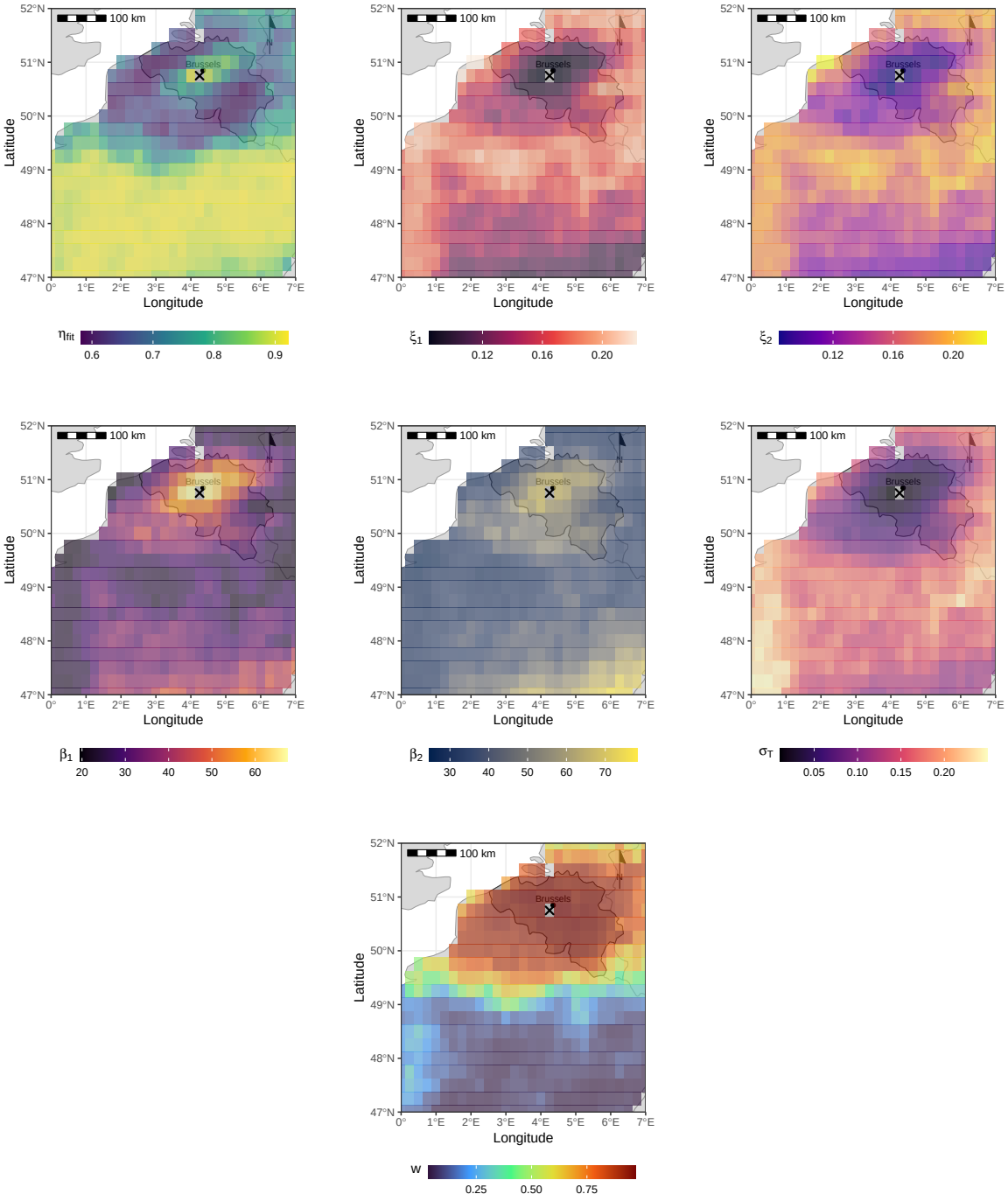

Figure A.7: Spatial fields of estimated dependence parameters of the sBGP model (Definition 3.1) for bivariate precipitation extremes between Brussels (reference location, black cross) and each grid point, obtained using the non-penalised NBE.

	Brussels–Nivelles	Ostend–Spa
η	0.77 (0.67, 0.85)	0.92 (0.84, 0.94)
ξ_1	0.09 (0.06, 0.14)	0.08 (0.07, 0.11)
ξ_2	0.08 (0.06, 0.13)	0.08 (0.07, 0.11)
β_1	47.11 (28.19, 65.55)	66.45 (49.17, 74.91)
β_2	60.46 (35.26, 74.40)	71.79 (52.62, 76.53)
σ_T	0.02 (0.02, 0.04)	0.07 (0.06, 0.10)
w	0.94 (0.89, 0.97)	0.10 (0.04, 0.29)

Table A.2: Parameter estimates (with 95% confidence intervals) for the sBGP model (Definition 3.1) fitted to the two representative pairs at the 70th-percentile threshold using the non-penalised NBE.

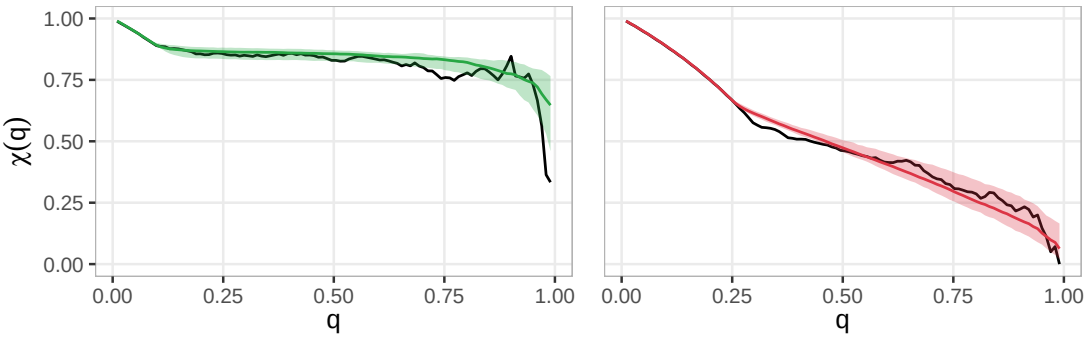

Figure A.8: Estimated $\chi_{\tilde{\mathcal{Z}}_{0.7}}(q)$ curves for Brussels–Nivelles and Ostend–Spa using the non-penalised NBE, where $\chi(q)$ is estimated using (3.5). Quantiles q are defined relative to the exceedance subset $\tilde{\mathcal{Z}}_{0.7}$ (i.e., within the exceedance region, $u_j = F_j^{-1}(0.7)$). The black line shows the empirical $\chi_{\tilde{\mathcal{Z}}_{0.7}}(q)$ from observed exceedances; the green and red lines are the model estimates; the shaded area denotes the 95% bootstrap confidence region.

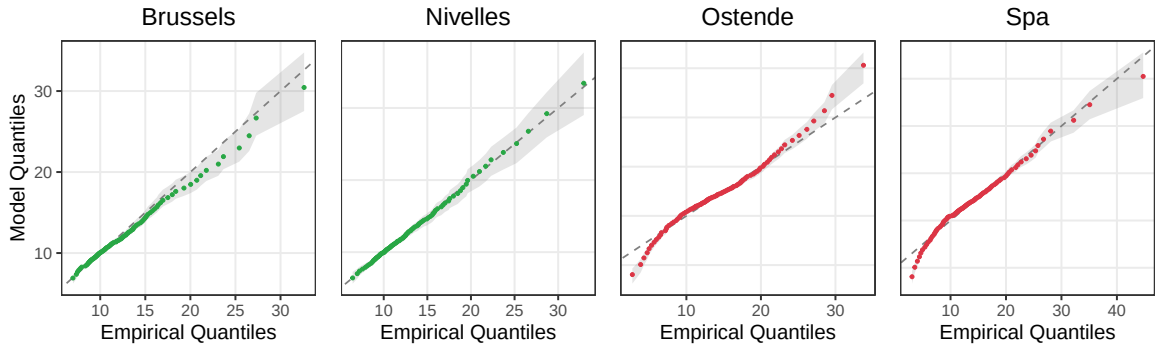

Figure A.9: QQ-plots comparing empirical marginal exceedances to fitted marginal distributions for Brussels–Nivelles and Ostend–Spa under the sBGP model (Definition 3.1) using the non-penalised NBE. Each panel corresponds to one margin of the respective pair. All plots are based on exceedances above the marginal threshold ($u_j = F_j^{-1}(0.7)$), with dashed vertical lines marking the threshold values. Theoretical quantiles are shown on the original data scale, obtained by adding the threshold to the modeled exceedances.

REFERENCES

Resnick, S. (2007). *Heavy-Tail Phenomena.* Springer.